Stability Charts for Uniform Slopes

Radoslaw L. Michalowski, F.ASCE[1]

Abstract: While computational tools have made most graphical methods and charts obsolete, stability charts for slopes are still routinely used in practice. The charts presented here are based on the kinematic approach of limit analysis that leads to a strict lower bound on stability number $c/\gamma H$ or an upper bound on the safety factor. An earlier suggestion is employed in this paper to produce charts that eliminate the necessity for iterations. Charts are presented for slopes subjected to pore water pressure and also for those exposed to seismic forces.

DOI: 10.1061/(ASCE)1090-0241(2002)128:4(351)

CE Database keywords: Slopes; Slope stability; Limit analysis; Limit states; Failures; Graphic methods.

Introduction

Stability assessments of earth slopes require limit state calculations, which differ significantly from those in structural engineering. This is because the weight of the soil constitutes the main load on slopes, yet it contributes to forces both resisting and driving the collapse. These forces depend on the mode of failure and the particular geometry of the failure mechanism. Consequently, the safety factor cannot be defined as a ratio of the limit load to the working load (both being ill-defined for slopes), but is usually defined as a function of the strength of the soil. Typically, the strength of the soil is described by the Mohr–Coulomb yield condition as a function of the cohesion, c, and the internal friction angle, φ. A common definition of the factor of safety (F) is the ratio of the shear strength of the soil to the shear stress necessary to maintain limit equilibrium

$$F=\frac{c}{c_d}=\frac{\tan\varphi}{\tan\varphi_d} \tag{1}$$

where c_d and φ_d are the soil strength parameters necessary only to maintain the structure in limit equilibrium. They are sometimes referred to as ''mobilized'' strength parameters. The factor in Eq. (1) is a ''global'' measure of safety and it ignores the progressive nature of most failure processes where the limit state is reached sequentially in the structure. Calculations of the safety factor require that parameters c_d and φ_d be used in analysis, independent of the technique used (finite element, limit analysis, etc.). Because c_d and φ_d are not true parameters of the soil, the analysis leads to a fictitious collapse mechanism that should not be interpreted as a true failure pattern. Despite this criticism, the safety factor as defined in Eq. (1) is generally accepted in practice, and it seems to be a reasonable measure of the safety of slopes.

[1]Professor, Dept. of Civil and Environmental Engineering, Univ. of Michigan, Ann Arbor, MI 48109-2125. E-mail: rlmich@umich.edu

Note. Discussion open until September 1, 2002. Separate discussions must be submitted for individual papers. To extend the closing date by one month, a written request must be filed with the ASCE Managing Editor. The manuscript for this technical note was submitted for review and possible publication on January 12, 2001; approved on August 29, 2001. This technical note is part of the ***Journal of Geotechnical and Geoenvironmental Engineering***, Vol. 128, No. 4, April 1, 2002. ©ASCE, ISSN 1090-0241/2002/4-351–355/$8.00+$.50 per page.

A large body of literature exists on the stability of slopes, and a comprehensive description of it was presented by Duncan (1996). No new analysis method is introduced in this paper, rather a convenient way of representing stability analysis results is revisited. The objective of this paper is to present convenient charts for estimations of safety factors, based on strict limit analysis (kinematic approach) calculations.

Stability Number

Analyses of stability of slopes with irregular inclination or with heterogeneous soils require the application of now computerized methods. However, charts for homogeneous slopes with a well defined inclination are often used in practice as a quick reference, and they are a convenient tool for the first estimate of the slope safety. An early example of such charts is the one produced by Taylor (1937). Taylor used the friction circle method (φ-circle method) to arrive at his chart. To present the results in a dimensionless manner he introduced a stability number defined as

$$N=\frac{c_d}{\gamma H}=\frac{c}{\gamma HF} \tag{2}$$

where γ = unit weight of soil and H = slope height. For $F=1$, the stability number in Eq. (1) represents the combination of c, γ, and H, which guarantees the slope to be at the verge of failure (limit equilibrium) for given slope inclination angle β and internal friction angle of the soil φ. The stability chart in Fig. 1 was produced using earlier computations based on the kinematic approach of limit analysis (Michalowski 1995), in which a log-spiral failure mechanism was utilized [Fig. 2(a)]. It seems that the stability number is nearly identical to that from Taylor's original chart.

The stability number for $\varphi=0$ becomes independent of the slope inclination when β is less than about 50°. This is an artifact of problem formulation with infinite soil depth, not just in the kinematic approach of limit analysis, but also in more approximate limit equilibrium techniques. This can be explained easily following limit analysis formulation. When $\varphi=0$ the failure surface becomes cylindrical [Fig. 2(b)], and the dimensions of the most adverse failure mechanism (for β less than about 50°) tend to infinity. Thus slope height H becomes negligible with respect to failure surface radius r. Consequently, the rate of work dissipation during collapse with rotational rate $\dot{\omega}$ about point O assumes a simple form [see Fig. 2(b) for α]

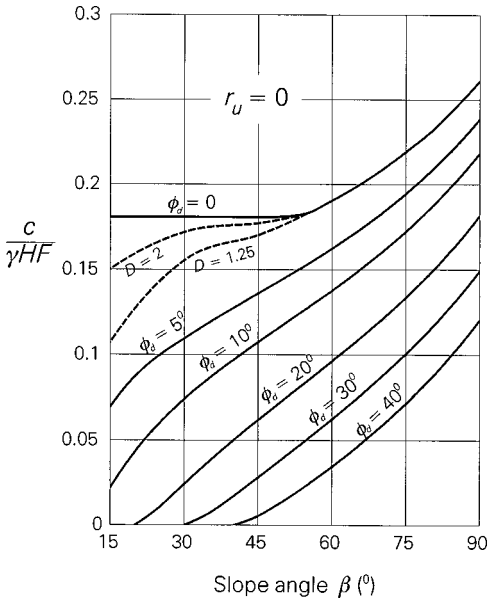

Fig. 1. Stability number for uniform slopes (limit analysis)

$$\dot{D} = cr^2\dot{\omega}(\pi - 2\alpha) \tag{3}$$

The center of rotation O is exactly above the midpoint of the slope [a point so clearly made by Fellenius (1927) for failure surfaces extending below the toe]. Hence the rate of the work of the slope weight, when $r \gg H$, becomes

$$\dot{W}_\gamma = \tfrac{1}{2}\gamma H\dot{\omega}r^2\cos^2\alpha \tag{4}$$

The integrated work rate of the soil weight below the slope is equal to zero (this is a direct consequence of the mass conservation principle and incompressibility of the soil; not true when $\varphi > 0$). Equating the dissipation rate in Eq. (3) to the work rate of the soil weight in Eq. (4) and solving for the stability number, one obtains

$$\frac{c}{\gamma H} = \frac{\cos^2\alpha}{2(\pi - 2\alpha)} \tag{5}$$

and the maximum of the stability number in Eq. (5) (best lower bound) is found when $\alpha \approx 23.2°$

$$\frac{c}{\gamma H} = 0.181 \tag{6}$$

The value in Eq. (6) is equal to that in Fig. 1 for $\varphi = 0$ and β less than about 50°. This result is not realistic, and this effect was already known to Taylor (1937). A more rational stability number is obtained by limiting the depth of the failure mechanism to a realistic value (for instance, equal to the depth of bedrock). Then, the approximation that slope height is negligible when compared to r ($r \gg H$) used in deriving Eqs. (3) and (4) is no longer valid, and the stability number becomes dependent on slope inclination angle β. Two dashed lines in Fig. 1 indicate the consequences of limiting the depth of the mechanism ($D = 2$ and $D = 1.25$). Depth factor D is explained in Fig. 2(c). In general, for steep slopes and large internal friction angles the most adverse failure surfaces intersect the slope toe, whereas for shallow slopes and soils with low φ below-the-toe surfaces yield the maximum stability number.

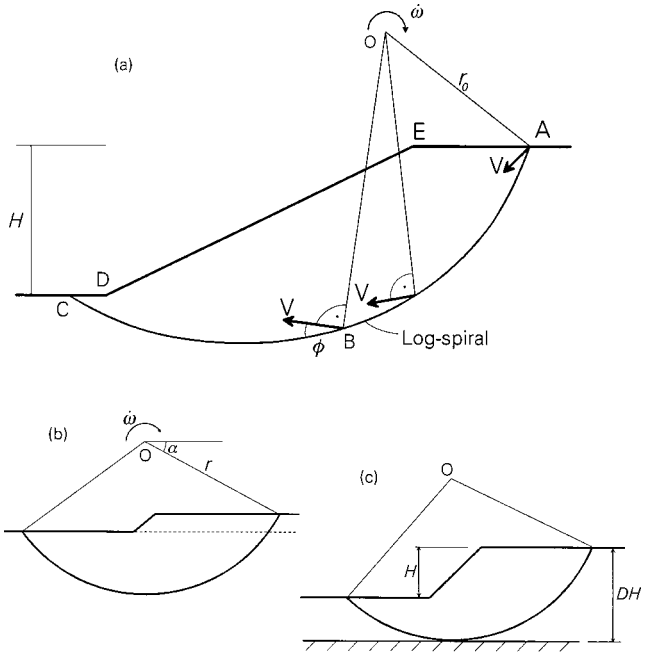

Fig. 2. Stability analysis: (a) rotational collapse mechanism; (b) large-size mechanism in cohesive soil; and (c) depth constraint

Based on the chart in Fig. 1, one can deduce the safety factor for a slope of given $c/\gamma H$, β, and φ. Because the safety factor must be applied to both c and $\tan\varphi$ [see Eq. (1)], the procedure of evaluating F from the chart in Fig. 1 is iterative (except for case $\varphi = 0$). There have been several attempts at constructing charts that require no iteration to evaluate the safety factor, among those: Bishop and Morgenstern (1960), Bell (1966), Singh (1970), and Cousins (1978), all of them based on some species of a slice method. Of these proposals the one suggested by Bell (1966) appears to be the most convenient.

The motivation for constructing the new charts was the presentation of a convenient tool for the quick assessment of the safety of slopes, based on the rigorous limit analysis approach. Bell (1966) proposed that $1/\tan\varphi_d$ (or $F/\tan\varphi$) be given as a function of $c_d/\gamma H\tan\varphi_d$ for a variety of inclination angles β. He referred to $c_d/\gamma H\tan\varphi_d$ as the modified stability number, N^*. The advantage of such representation is that parameter N^* is independent of safety factor F

$$N^* = \frac{c_d}{\gamma H\tan\varphi_d} = \frac{c/F}{\gamma H(\tan\varphi/F)} = \frac{c}{\gamma H\tan\varphi} \tag{7}$$

Hence estimation of the safety factor from charts presented as functions of N^* will not require any iterative procedures. One might argue that N^* should no longer be called a stability number, since it only contains information about the soil and slope geometry, not the stability. Bell (1966) used his concept to redraw Taylor's chart and also to present some additional results from Bishop's slice method computations. More recently, Baker and Tanaka (1999) revisited this concept drawing attention to this useful method of presenting results of slope stability analyses.

Of course, stability charts developed in terms of N^* cannot be used for slopes with zero internal friction angle, in which case the expression in Eq. (7) becomes singular.

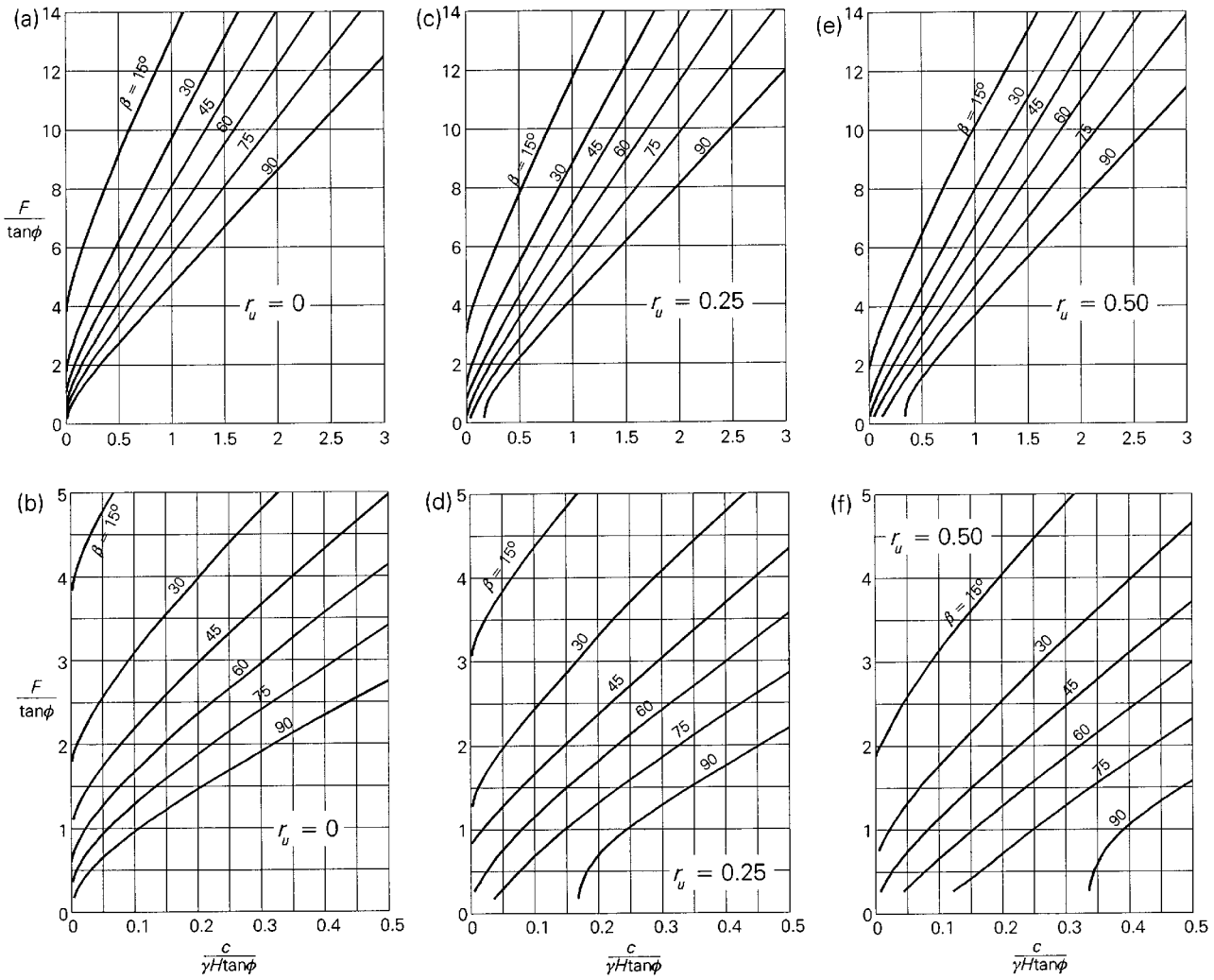

Fig. 3. Stability charts for uniform slopes

Stability Analysis

The charts are developed here using the kinematic approach of limit analysis applied to a rigid rotation collapse mechanism. The failing soil mass is separated from the soil at rest by log-spiral failure surface ABC, Fig. 2(a). An early proposal of this mechanism was suggested by Rendulic (1935), who obtained a closed-form solution to a moment due to shear resistance along a sector of a log-spiral. As was proved later, rigid rotation of a block separated by a log-spiral surface is a kinematically admissible mechanism from the limit analysis standpoint, and it leads to a strict lower bound on stability number $c/\gamma H$. Taylor (1937) was well aware of the Rendulic proposal, but he chose to develop his charts based on the friction circle method, as it lends itself better to a graphical technique of solution (not surprising, considering the year of development of these charts).

The limit analysis based on the log-spiral mechanism for simple slopes was proposed by Chen et al. (1969). Subsequently, the influence of pore water pressure, seismic effects, and soil reinforcement were included in the analysis (Michalowski 1995, 1998, 1999). Computer programs for calculations of pore water pressure and quasi-static seismic effects developed earlier were modified to produce the charts presented in this paper.

Stability Charts for Slopes Subjected to Pore Pressure

The two effects that must be accounted for in the case of the presence of water are the buoyancy and seepage forces. In limit equilibrium calculations these can be included in two ways: (1) using the saturated (total) unit weight of the soil and accounting for water forces on the boundaries of moving blocks, or (2) using the buoyant unit weight with seepage forces in the soil skeleton. In either case, the strength of the soil is considered in terms of effective stress. In the kinematic approach of limit analysis the presence of water must be considered through work terms in the energy (rate) balance equation. To do this effectively, the pore water pressure is considered as a body force, similar to gravity or magnetic forces. In the process of deformation (failure) frictional soils dilate and the pore water pressure does work on the volumetric strain of the soil skeleton, similar to the work of air pressure acting on a balloon shell during expansion of that shell. This work can be proved to contain the effects of buoyancy and seepage forces, and this approach was used to obtain stability numbers for slopes subjected to pore water pressure (Michalowski 1995). Theoretical underpinning of this approach was reiterated step-by-step in Michalowski (1999). The incipient collapse process is con-

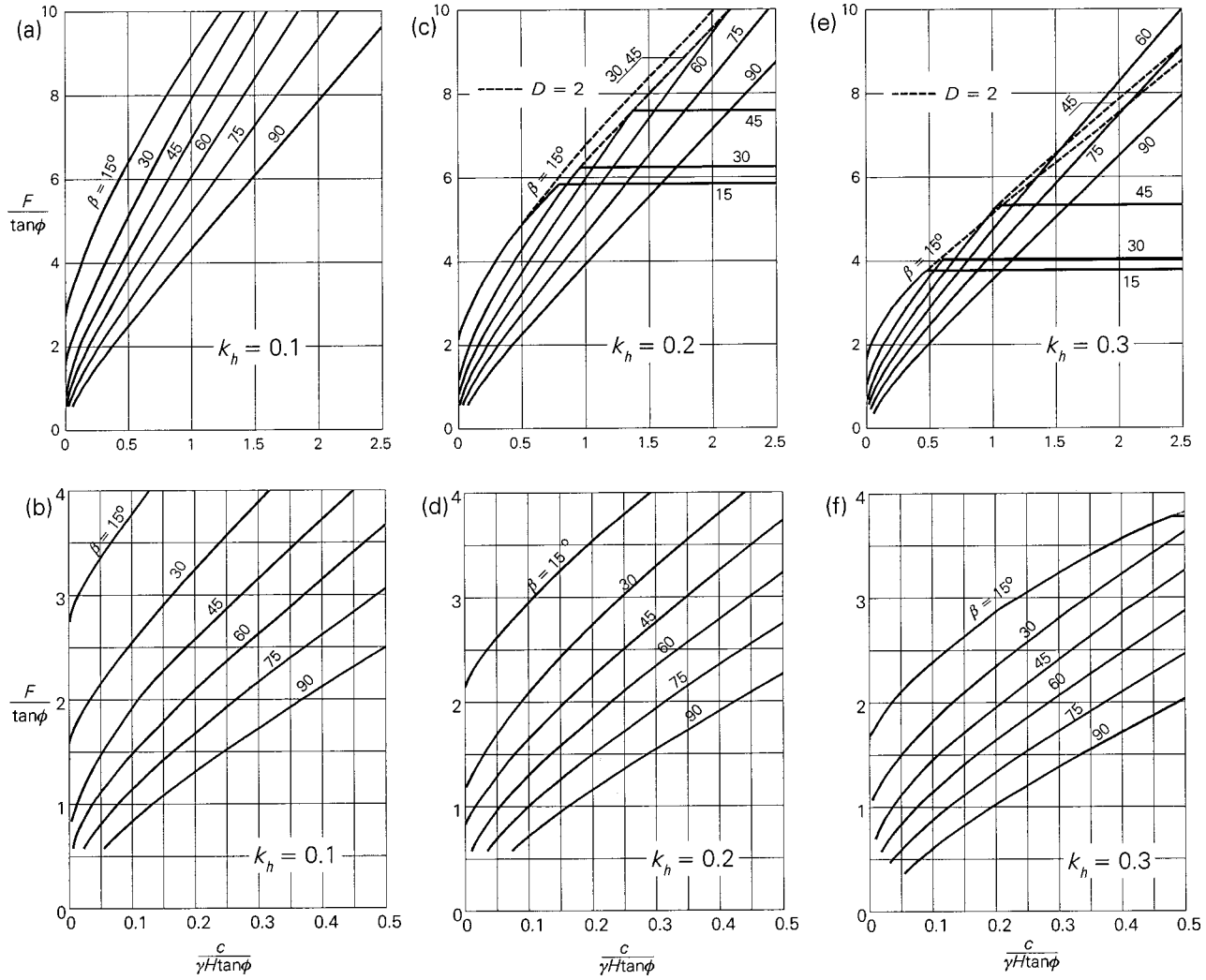

Fig. 4. Safety factor for slopes subjected to quasi-static horizontal force

sidered to be fully drained where dilation of the soil skeleton does not cause any change in the magnitude of the pore water pressure.

For the purpose of presenting the influence of the pore water on the stability of slopes, the distribution of the pore water pressure is described by coefficient r_u defined by Bishop and Morgenstern (1960) as

$$r_u = \frac{u}{\gamma h} \tag{8}$$

where u = magnitude of the pore water pressure, γ = soil unit weight, and h = depth of the point on the failure surface below the slope surface. Stability charts for slopes with r_u equal to 0, 0.25, and 0.50 are presented in Fig. 3. The data in the charts in Fig. 3 was created using a computer program written earlier (Michalowski 1995).

Coefficient r_u is a rather crude manner of accounting for the pore water pressure in a slope. If a well-defined flow net in a slope is known, the corresponding pore pressure distribution can be calculated and included explicitly in computations of the stability number (or the safety factor). While such calculations are more accurate, presentation of the results in charts would be difficult because of the large number of variables needed to describe realistic flow nets. While the nature of calculations with pore pressures described in Eq. (8) is rather approximate, the results make it possible to make an ''educated guess'' of the influence of pore water pressure on the stability of slopes.

Quasi-Static Seismic Effect

Seismic loads on slopes are often considered in design by including quasi-static forces due to seismic acceleration. While such an analysis ignores the seismic process (acceleration history) and does not give any insight into the behavior of the structure, it is routinely used in design. The kinematic approach of limit analysis was used here to arrive at the data used to produce the charts in Fig. 4. Coefficient k_h represents the intensity of horizontal acceleration as a fraction of the gravity acceleration. The effect of quasi-static forces was included in the analysis as an additional work term in the energy balance equation (Michalowski 1998).

No pore water pressure was considered in calculations with a quasi-static seismic force. The quasi-static approach is a crude approximation of seismic effects, and charts involving another simplified concept (r_u) to describe the pore water pressure distribution, in addition to k_h, may not be indicative of the true safety margin of slopes. Such charts would be an inappropriate tool for analyzing the safety of slopes, particularly for liquefiable soils.

Safety factor F, represented in the charts as $F/\tan\varphi$, is an increasing function of N^* (or $c/\gamma H \tan\varphi$) up to some threshold

value, beyond which the safety factor becomes independent of parameter N^*. This leads to a counterintuitive conclusion that the safety factor becomes independent of the cohesion. For $k_h=0.1$ this happens beyond the range presented in Fig. 4(a), but this effect is present on the charts in Figs. 4(c and e) for slopes with an inclination of 15–45°. This is an artifact of the problem formulation with an infinite extent of the soil, similar to that indicated earlier for the chart where $\varphi=0$ in Fig. 1. Here, this effect can be explained by analyzing the tendency of various terms in the energy balance equation applied to incipient deformation of a deep collapse mechanism.

The predominant force resisting collapse is equal to the mobilized strength along the failure surface, whereas the predominant force driving the collapse is the quasi-static force due to earthquake acceleration. For the plane-strain mechanism considered here, the resisting force is proportional to a characteristic length (size) of the mechanism [for instance, r_0, Fig. 2(a)], while the driving force is proportional to the square of the characteristic length (the soil weight term, although also proportional to the square of the mechanism dimension, increases at a slower rate with an increase in the mechanism size). Consequently, for any slope of inclination β subjected to some horizontal acceleration one can determine internal friction φ of the soil such that stability number $c/\gamma H$ tends to infinity when the mechanism tends to infinite size (critical height of the slope becomes zero or infinite cohesion is needed to maintain limit equilibrium). Applying constant k_h to a very large mass of soil is, of course, unreasonable. As before, the outcome is not realistic, and more reasonable results were found when the mechanism was limited to some realistic depth.

Calculation results are presented as dashed lines in Figs. 4(c and e) for mechanisms of limited depth, with a depth-to-height ratio $D=2$. When $k_h=0.2$ [Fig. 4(c)], the dashed lines for $\beta=30°$ and 45° nearly overlap, whereas for $k_h=0.3$ a curve for $\beta=30°$ is not shown to preserve the clarity of the chart.

Example

Let a 10 m tall slope with a 30° inclination be comprised of soil whose $\varphi=20°$, $c=10$ kN/m^2, and $\gamma=17$ kN/m^3. Evaluating a safety factor for this slope using the chart for stability number $c/\gamma H$ (Fig. 1) has to be done iteratively. Taking the initial guess of the safety factor for the first iteration as $F=1.5$ we have $\varphi_d \approx 13.6°$ [from Eq. (1)], and, interpolating from the chart: $c/\gamma HF \approx 0.07$, hence $F=(c/\gamma H)/0.07 \approx 0.84$. Taking the second guess as $F=1.4$ and following a similar procedure, we arrive at the value $F \approx 1.17$, and in the third iteration the procedure converges at $F \approx 1.3$.

Now, using the new charts, we first calculate $c/\gamma H \tan\varphi = 0.162$. From the chart in Fig. 3(b) for $\beta=30°$ we read $F/\tan\varphi \approx 3.6$, hence $F=3.6\cdot\tan 20° \approx 1.3$. However, this slope would approach the verge of failure if either it was subjected to pore pressures equivalent to those described by $r_u=0.25$, or it was subjected to a quasi-static horizontal force equivalent to $k_h=0.1$.

Conclusions

A set of charts was produced for assessment of the stability of slopes. The data was obtained from the calculations based on the kinematic approach of limit analysis. The charts can be used for slopes subjected to pore water pressure and those exposed to horizontal (possibly seismic) forces. They are convenient to use, and evaluating the safety factor does not require an iterative process. However, these charts are not intended for slopes in soils with a zero frictional component of strength.

Acknowledgment

The writer was supported by the National Science Foundation, Grant No. CMS-0096167, when working on the subject presented in this paper. This support is greatly appreciated.

References

Baker, R., and Tanaka, Y. (1999). ''A convenient alternative representation of Taylor's stability charts.'' *Proc., Int. Symposium on Slope Stability Engineering*, Balkema, Rotterdam, Vol. 1, 253–257.

Bell, J. M. (1966). ''Dimensionless parameters for homogeneous earth slopes.'' *J. Soil Mech. Found. Div., Am. Soc. Civ. Eng.*, 92(5), 51–65.

Bishop, A. W., and Morgenstern, N. R. (1960). ''Stability coefficients for earth slopes.'' *Geotechnique*, 10(4), 129–150.

Chen, W. F., Giger, M. W., and Fang, H. Y. (1969). ''On the limit analysis of stability of slopes.'' *Soils Found.*, 9(4), 23–32.

Cousins, B. F. (1978). ''Stability charts for simple earth slopes.'' *J. Geotech. Eng. Div., Am. Soc. Civ. Eng.*, 104(2), 267–279.

Duncan, J. M. (1996). ''State of the Art: Limi equilibrium and finite-element analysis of slopes.'' *J. Geotech. Eng., Am. Soc. Civ. Eng.*, 122(7), 577–596.

Fellenius, W. (1927). *Erdstatische Berechnungen mit Reibung und Kohäsion (Adhäsion) und unter Annahme kreiszylindrischer Gleitflächen*, Ernst & Sohn, Berlin.

Michalowski, R. L. (1995). ''Slope stability analysis: a kinematical approach.'' *Geotechnique*, 45(2), 283–293.

Michalowski, R. L. (1998). ''Soil reinforcement for seismic design of geotechnical structures.'' *Comp. Geotechn.*, 23(1), 1–17.

Michalowski, R. L. (1999). ''Stability of uniformly reinforced slopes. Closure.'' *J. Geotech. Geoenviron. Eng.*, 125(1), 84–86.

Rendulic, L. (1935). ''Ein betrag zur bestimmung der gleitsicherheit.'' *Der Bauingenieur*, 16(19/20), 230–233.

Singh, A. (1970). ''Shear strength and stability of man-made slopes.'' *J. Soil Mech. Found. Div., Am. Soc. Civ. Eng.*, 96(6), 1879–1892.

Taylor, D. W. (1937). ''Stability of earth slopes.'' *J. Boston Soc. Civil Eng.*, 24(3). Reprinted in: *Contributions to Soil Mechanics 1925 to 1940*, Boston Society of Civil Engineers, 337–386.